Modeling the impact of solid noise barriers on near road air quality

Article *in* Atmospheric Environment · July 2016

DOI: 10.1016/j.atmosenv.2016.07.005

4 authors, including:

Akula Venkatram
University of California, Riverside
166 PUBLICATIONS **2,812** CITATIONS
SEE PROFILE

Parikshit Deshmukh
Jacobs Engineering Group Inc
6 PUBLICATIONS **61** CITATIONS
SEE PROFILE

Richard William Baldauf
United States Environmental Protection Age…
91 PUBLICATIONS **1,209** CITATIONS
SEE PROFILE

Atmospheric Environment 141 (2016) 462–469

Contents lists available at ScienceDirect

Atmospheric Environment

journal homepage: www.elsevier.com/locate/atmosenv

Modeling the impact of solid noise barriers on near road air quality

Akula Venkatram [a], Vlad Isakov [b], Parikshit Deshmukh [c], Richard Baldauf [d, e, *]

[a] University of California, Riverside, CA, USA
[b] U.S. EPA, Office of Research and Development, National Exposure Research Laboratory, Atmospheric Modeling and Analysis Division, Research Triangle Park, NC, USA
[c] Jacobs Technology, Durham, NC, USA
[d] U.S. EPA, Office of Research and Development, National Risk Management Research Laboratory, Research Triangle Park, NC, USA
[e] U.S. EPA, Office of Transportation and Air Quality, National Vehicle and Fuels Emissions Laboratory, Ann Arbor, MI, USA

HIGHLIGHTS

- Developed a dispersion model algorithm for noise barriers in unstable meteorology.
- Account for the lofting of the plume above the height of the barrier.
- Simulate the entrainment of the elevated plume into the cavity behind the barrier.
- Model compared to field measurement data in Phoenix, Arizona, USA.
- Model predicted reductions similar, but slightly lower, than field measurements.

ARTICLE INFO

Article history:
Received 9 June 2015
Received in revised form
28 June 2016
Accepted 1 July 2016
Available online 8 July 2016

Keywords:
Air quality
Dispersion model
Noise barrier
Field data
Emission factors

ABSTRACT

Studies based on field measurements, wind tunnel experiments, and controlled tracer gas releases indicate that solid, roadside noise barriers can lead to reductions in downwind near-road air pollutant concentrations. A tracer gas study showed that a solid barrier reduced pollutant concentrations as much as 80% next to the barrier relative to an open area under unstable meteorological conditions, which corresponds to typical daytime conditions when residents living or children going to school near roadways are most likely to be exposed to traffic emissions. The data from this tracer gas study and a wind tunnel simulation were used to develop a model to describe dispersion of traffic emissions near a highway in the presence of a solid noise barrier. The model is used to interpret real-world data collected during a field study conducted in a complex urban environment next to a large highway in Phoenix, Arizona, USA. We show that the analysis of the data with the model yields useful information on the emission factors and the mitigation impact of the barrier on near-road air quality. The estimated emission factors for the four species, ultrafine particles, CO, NO_2, and black carbon, are consistent with data cited in the literature. The results suggest that the model accounted for reductions in pollutant concentrations from a 4.5 m high noise barrier, ranging from 40% next to the barrier to 10% at 300 m from the barrier.

Published by Elsevier Ltd.

1. Introduction

With a growing number of studies linking population exposures to nearby traffic emissions with adverse health effects (e.g. summary by Health Effects Institute, 2010), interest has increased in identifying methods to mitigate these impacts. One approach that has received recent attention is the use of roadway design to reduce near-road pollution concentrations. The designs include roadside noise barriers, roadside vegetation, and elevated or depressed roadways (Baldauf et al., 2009). Field measurements have shown that solid roadside noise barriers have the potential to reduce downwind pollutant concentrations (Baldauf et al., 2008; Ning et al., 2010; Hagler et al., 2012). Wind tunnel simulations (Heist et al., 2009); computational fluid dynamics modeling (Hagler et al., 2011); and tracer gas studies (Finn et al., 2010) also indicated that solid roadside barriers represent practical mitigation

* Corresponding author.U.S. EPA, Office of Research and Development, National Risk Management Research Laboratory, Research Triangle Park, NC, USA.
E-mail address: Baldauf.Richard@epa.gov (R. Baldauf).

http://dx.doi.org/10.1016/j.atmosenv.2016.07.005
1352-2310/Published by Elsevier Ltd.

methods that can result in substantial reductions in pollutant concentrations caused by line source emissions, such as those from traffic, relative to those in the absence of barriers.

Schulte et al. (2014) initially developed a semi-empirical dispersion model to estimate the impact of solid barriers on pollutant transport and dispersion using data from the tracer study described by Finn et al. (2010). This paper uses a modified version of the Schulte et al. (2014) model to interpret data from a field study conducted in the vicinity of an urban highway in Phoenix, Arizona, USA (Baldauf et al., 2016). The field study in Phoenix provides a real-world evaluation of solid barrier effects, where we expect a multitude of confounding factors that are absent in a controlled tracer study. The Phoenix data was collected during daytime using a mobile platform that measured concentrations of several pollutants on the highway and at distances of up to 300 m away from the road, both with and without a solid barrier present. The reductions in concentrations associated with the 4.5 m high noise barrier ranged from 40% to 50% relative to concentrations measured along the same stretch of highway in the absence of the barrier.

2. Modified barrier model

Wind tunnel observations (Heist et al., 2009) and computational fluid dynamics modeling (Hagler et al., 2011) indicate that the major effects of solid barriers on downwind pollutant concentrations are: 1) pollutants emitted from the road become well-mixed in a zone extending from the ground to the barrier height and this mixing persists downwind over several barrier heights 2) turbulent velocities are increased downwind of the barrier, and 3) the pollutant plume is lofted above the top of the barrier, which results in a concentration maximum above the top of the barrier.

Schulte et al. (2014) developed a semi-empirical dispersion model that incorporated some of the observed effects induced by barriers on dispersion. The model assumes that the pollutant is well mixed below the height of the wall. This assumption coupled with the increase in turbulence by the wall provided an adequate description of the data from the wind tunnel (Heist et al., 2009) and tracer studies Finn et al. (2010) during near neutral conditions. However, the model overestimated concentrations close to the barrier under unstable conditions.

In this paper, we modify the model of Schulte et al. (2014) to reduce the overestimation close to the barrier. First, we loft the plume maximum above the wall as observed in the wind tunnel. Second, we reduce the entrainment of the elevated plume into the wake of the wall through a function that depends on stability characterized by the Monin-Obukhov length.

The model is based on the Gaussian plume formulation for the concentration $C(x,z)$ from an infinite line source:

$$C(x,z) = C_{\max}\left[\exp\left(-\frac{1}{2}\left(\frac{z-h_p}{\sigma_z}\right)^2\right) + \exp\left(-\frac{1}{2}\left(\frac{z+h_p}{\sigma_z}\right)^2\right)\right] \quad (1)$$

where h_p is the effective plume height. Equation (1) defines the profile of the concentration above the well mixed region that extends below the wall height, h_w. Below h_w, the concentration is well mixed and is denoted by C_s,

$$C_s = f_m C(x, z = h_w), \quad (2)$$

where h_w is the wall height, and f_m is an entrainment coefficient we will parameterize later.

We compute C_{max} by conserving the horizontal flux of material:

$$\left(U_w C_s h_w + U_e \int_{h_w}^{\infty} C(x,z)dz\right)\cos\theta = q, \quad (3)$$

Where q is the emission rate of the line source, U_w is the velocity in the well mixed region, which is taken to be the value at $z = h_w$, U_e is the effective transport velocity of the plume material above the wall height and θ is the angle between the mean wind and the normal to the line source. Note that σ_z in Equation (1) is evaluated at $x/cos\theta$, where x is the perpendicular distance of the receptor from the line source. The vertical spread,σ_z, and the effective velocity, U_e, are estimated using the formulations described in Schulte et al. (2014).

The first term on the left hand side of Equation (2) is the mass being transported below the wall, and the second term is the mass transported above the wall. Substituting Equations (1) and (2) into (3) yields the expression for C_{max},

$$C_{\max} = q\Big/\Big(\cos\theta\Big(h_w U_w f_m\Big(\exp\Big(-p_1^2\Big) + \exp\Big(-p_2^2\Big)\Big) + U_e\sigma_z(2 - erf(p_1) - erf(p_2))\Big)\Big), \quad (4)$$

where erf is the error function, and

$$p_1 = \left(\frac{h_w - h_p}{\sqrt{2}\sigma_z}\right),\ p_2 = \left(\frac{h_w + h_p}{\sqrt{2}\sigma_z}\right). \quad (5)$$

Then, C_s, the ground-level concentration can be calculated from Equation (2) once the entrainment factor, f_m, is specified.

In Schulte et al. (2014), we took $f_m = 1$ in Equation (2), and the plume height, $h_p = h_w$, which implies that the plume concentration decreases above the wall. In the modified model, we loft the plume above the wall by taking $h_p = h_w + \sigma_z/2$, where the plume properties correspond to the modified micrometeorology after the wall. We now allow f_m to be small next to the wall to reduce the wall's mixing effect during unstable conditions. The entrainment factor is parameterized as

$$f_m = f_c + (1 - f_c)(1 - \exp(-x/L_s)), \quad (6)$$

where the entrainment factor, f_c, at $x = 0$ is taken to be a function of the Monin-Obukhov length, L_{MO},

$$f_c = \exp(-L_s/|L_{MO}|), \quad (7)$$

Equation (6) is designed to allow the entrainment factor to approach unity over a length scale, $L_s = 10h_w$. The factor, f_c, ensures that the entrainment into the cavity behind the wall decreases as $|L_{MO}|$ decreases: the entrainment decreases as the surface layer becomes more unstable.

We account for the effect of the finite length of the source using the approximation described in Venkatram and Horst (2006). In applying the model to a highway, we assume that the center of each lane is a line source, and the traffic flow is distributed equally among the lanes.

3. Evaluation with Idaho Falls field study

The set of parameterizations described here were obtained by comparing model estimates to observations made in the Idaho Falls tracer experiment, details of which are described in Finn et al. (2010). In brief, the field study was conducted in 2008 near NOAA's Grid 3 diffusion grid at the Department of Energy's Idaho

National Laboratory (INL). A 90 m long by 6 m high straw bale stack represented a roadway barrier for the primary experiment. The "roadway" was an access track through the sagebrush adjacent to the barrier. The primary and reference control experiments both had a 54 m long (9H) SF_6 tracer line source release positioned 1 m above ground level (AGL) representing pollution sources from a roadway. In the primary experiment, the line source was positioned 1 m upwind of the 6 m high barrier with a gridded array of bag samplers downwind of the line source and barrier for measuring mean 15-min concentrations. The control experiments (conducted at an adjacent location and simultaneous to the primary) include identical source and concentration sampling but without the barrier in the array.

Test 1 was conducted on October 9, 2008 from 1230 to 1530 h Mountain Standard Time (MST) in neutral stability conditions. Test 2 was conducted on October 17, 2008 from 1300 to 1600 h MST in unstable conditions. Test 3 was conducted on October 18, 2008 from 1600 to 1900 h MST in weakly stable conditions. Test 5 was conducted on October 24, 2008 from 1800 to 2100 h MST in moderate to strongly stable conditions. The model described in Schulte et al. (2014) overestimated the concentrations during Test 2, conducted under unstable conditions.

Fig. 1 shows that the modified model reduces the problem with overestimating maximum concentrations near the barrier under unstable conditions. We realize that parameterizations in the model do not represent explanations of the underlying physical mechanisms. On the other hand, the empirical performance of the model shown in Fig. 1 suggests that they might be useful in modeling the impact of barriers under unstable conditions.

4. Evaluation with phoenix field study data

The field study was conducted along two highway segments along Interstate-17 (I-17) in Phoenix, Arizona, USA over one month covering October and November 2014 as described in detail by Baldauf et al. (2016). One segment was located on the west side of the highway and the other on the east side of the highway. Each segment was approximately 2 km in length and 500 m in width. The highway was at-grade with the surrounding terrain and contained sections with and without noise barriers along the same stretch of limited-access highway. The noise barriers along each segment were approximately 4.5 m in height, less than 1 m in thickness, approximately 3 m from the nearest travel lane of I-17, and had an access road immediately behind the wall. The area downwind of the noise barriers was residential, while downwind of the open section contained more commercial land use.

We focused on concentrations only when the wind was from the east and the sampling was performed on the west section of the freeway. We did not have a sufficient number of simultaneous meteorological and concentration measurements from the east section sampling to obtain meaningful modeling results.

Fig. 2 shows an aerial view and a map of the sampling route of the mobile monitoring vehicle in the west segment. This figure highlights the portion of the route behind the barrier and along the open section. The access road was parallel to I-17 except for the southern end, as seen in the 0–200 m North-South grid of the open section in Fig. 2. At this end, the access road gradually increased in distance away from the highway as it merges with the ramp coming off I-17 and ending at the east-west cross-street. The majority of this study area was also at-grade with the highway; however, the elevation of the access road at the southern end had a gradual rise in height above the level of I-17 to reach the elevation of the east-west cross-street.

Air quality measurements consisted of black carbon (BC), ultrafine particles (UFP), nitrogen dioxide (NO_2), and carbon monoxide (CO) using mobile monitoring in the open section and behind the 4.5 m solid noise barrier. An SUV also measured BC, UFP, NO2, and CO at a fixed-site location in the open section for quality assurance purposes. Sonic anemometers were placed at on a tower at heights of 1.8, 2.7 and 3.7 m above ground at a fixed-site behind the barrier. A fourth sonic anemometer was placed next to the SUV at 3 m above ground to obtain wind flows in the open location.

Data from these sonic anemometers were used to construct inputs to the model described in the previous section. Meteorological inputs for the no-barrier (open) concentration estimates were derived from the 3 m high sonic next to the SUV. Data from the 2.7 m sonic behind the barrier were used to compute concentrations downwind of the barrier using meteorological data measured during the same period.

The traffic flow information described in Baldauf et al. (2016) was multiplied by an emission factor to derive the emission rate estimates for the model. The values of the emission factors and the effective background concentrations were uncertain. So, their values were treated as parameters that provided the best fits between model estimates and concentrations measured behind the barrier. We did not fit model estimates to concentrations downwind of the open section because, as reported in Baldauf et al. (2016), the open section roads may have been impacted by

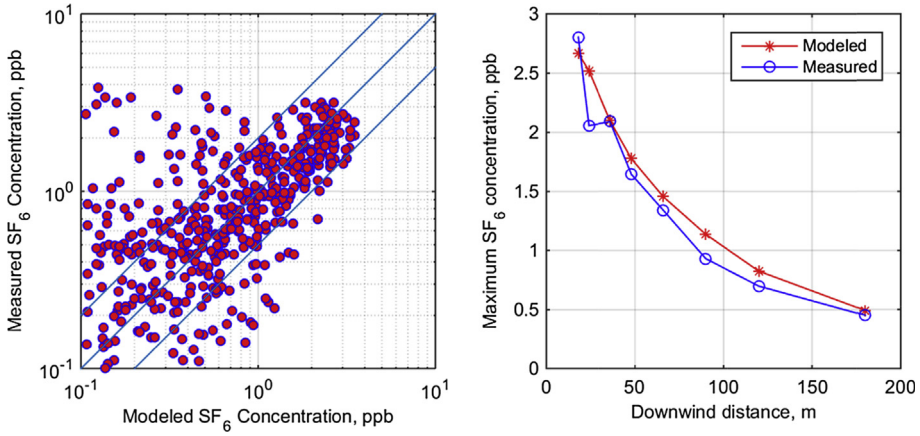

Fig. 1. The left panel is a scatter plot comparing modeled and measured tracer concentrations at the 58 receptors on the receptor grid with a barrier. The concentrations correspond to 15-min averages from experiments when the surface layer was unstable. The right panel is the average of the maximums observed at each downwind distance.

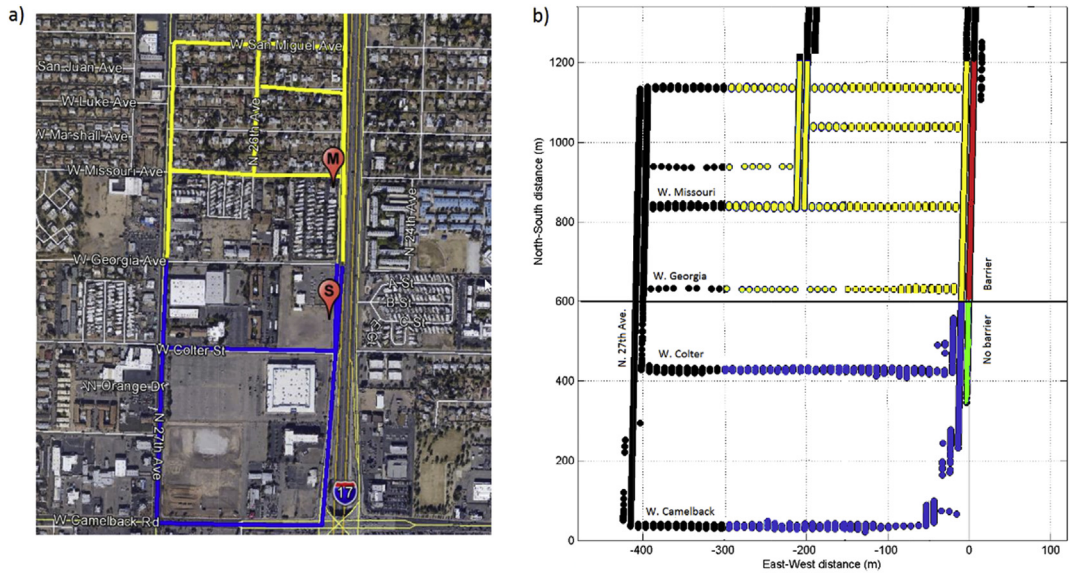

Fig. 2. Aerial view (a) and schematic map (b) of the Phoenix study area showing locations of mobile sampling route in the west section. The portion of the route behind the barrier is shown in yellow while the portion in the open section is shown in blue. The on-road portion of the route in front of the barrier is shown in red and in front of the open section in green on the schematic map. The "S" pin shows the location of the fixed-site SUV sampling platform, and the "M" pin the portable sampling tower. (For interpretation of the references to colour in this figure legend, the reader is referred to the web version of this article.)

vehicular traffic on the arterial road to the south which supported commercial land use. These traffic emissions likely contributed to the open section measurement values, but could not be readily included in the modeling described in this paper.

The data from the mobile monitor were assigned into bins of distances to allow averaging of the concentrations measured in each bin. The bins were 0–50 m, 50–90 m, 90–150 m, 150–250 m and 250–350 m, which provided the spatial resolution required to compare model estimates to observations close to the barrier, and at the same time have sufficient data for deriving averages. The analysis was performed with time periods that had simultaneous measurements of concentrations, meteorology, and traffic flow. This resulted in about 22 h of data for analysis.

The meteorological inputs were derived from 1 Hz data averaged over 15-min intervals. Pollutant concentrations were modeled for each of these intervals and then aggregated to produce the average over the entire sampling period. The model estimates correspond to the midpoints of these distance bins used to aggregate the measured concentrations. Assuming that the 15-min averaged concentrations represent independent samples, we estimated the standard error in the mean as the standard deviation of the 15-min averages in each bin divided by the square root of the sample size ($n = 88$). The standard errors of the measured values were estimated as the standard deviation of 15-min averaged concentrations derived from the sequence of 1-s sampled values, divided by the square root of the size of the sample. However, unlike the modeled values, these samples are distributed over the study region downwind of the highway. So, in order to estimate the standard error of the measured mean in each distance bin, we assumed that the ratio of the standard error to the mean (coefficient of variation) of the entire set of 88 measured samples remained constant across the bins. This, then allowed us to estimate the standard error of the measured mean, corresponding to 88 samples, in each distance bin. The 95% confidence intervals of the means of the measured and estimated concentrations were estimated by assuming that they are log-normally distributed about the overall mean in each distance bin.

5. Results and discussion

All pollutant measurements were compared to model estimates for the Phoenix field study data. Fig. 3 compares the modeled BC concentrations with observations. The left panel indicates that observed BC concentrations downwind of the open section appear to be impacted by sources not accounted for in the model: the concentration gradient is relatively flat from 100 to 200 m. This impact of emissions from the traffic to the south and downwind of the open section is also evident in Figs. 4–6 corresponding to concentrations of UFP, CO, and NO_2.

We also see the effects of the data collected on the access road in the 0–50 m zone from the road (corresponding to the 0–200 m North-South section in Fig. 2). The measured concentrations in this 0–50 m distance from the road, downwind of the open section, are close to those measured downwind of the barrier section. This result is likely because more measurements occurred closer to the outer edge of the 0–50 m bin and many of these measurements were at elevations above the freeway. As shown in a study in Las Vegas, Nevada, USA (Baldauf et al., 2013), near-road measurements collected above the grade of the highway can be lower than a corresponding at-grade measurement, especially for peak pollution levels.

As expected, model results do not compare as well with observations in the open section as seen in the bottom left panel of the figure because of the complexity of this portion of the sampling route. The measured concentrations show relatively flat gradients and are much higher than the modeled values at most distances from the road likely due to traffic emissions from the road to the south. In the 0–50 m zone from the road, the modeled concentrations are higher than the measurements presumably because a fraction of the measurements correspond to further distances from the road and collection at elevations above the highway.

Figs. 3–6 show that the model provides good descriptions of the concentrations measured downwind of the barrier presumably because the measurements are not affected by emissions along the sampling path. The mean values and the 95% confidence intervals of the background concentrations and emission factors, obtained by

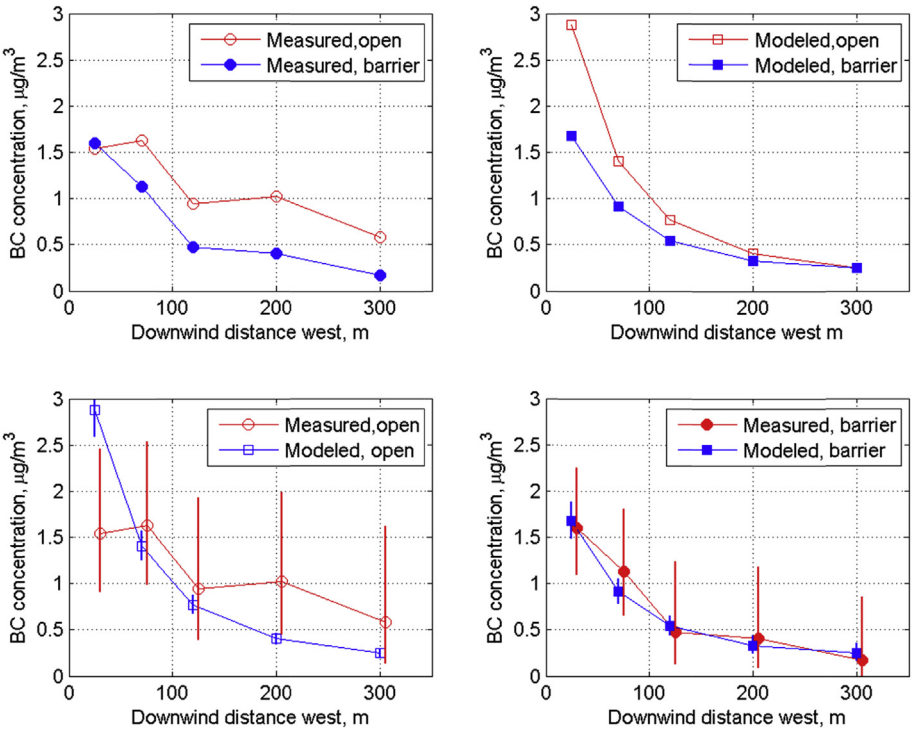

Fig. 3. Comparison of modeled and measured black carbon (BC) concentrations from measurements collected on the west section of I-17 in Phoenix, Arizona: **Top left panel**: Measured concentrations downwind of the open and barrier sections of the road. **Top right panel**: Measured concentrations downwind of the open and barrier sections of the road. **Bottom left panel**: Modeled concentrations downwind of the open section compared with measurements, **Bottom right panel**: Modeled concentrations downwind of the barrier section compared with measurements. Estimated background concentration is subtracted from the measured values. The vertical lines in the bottom panels correspond to the 95% confidence interval.

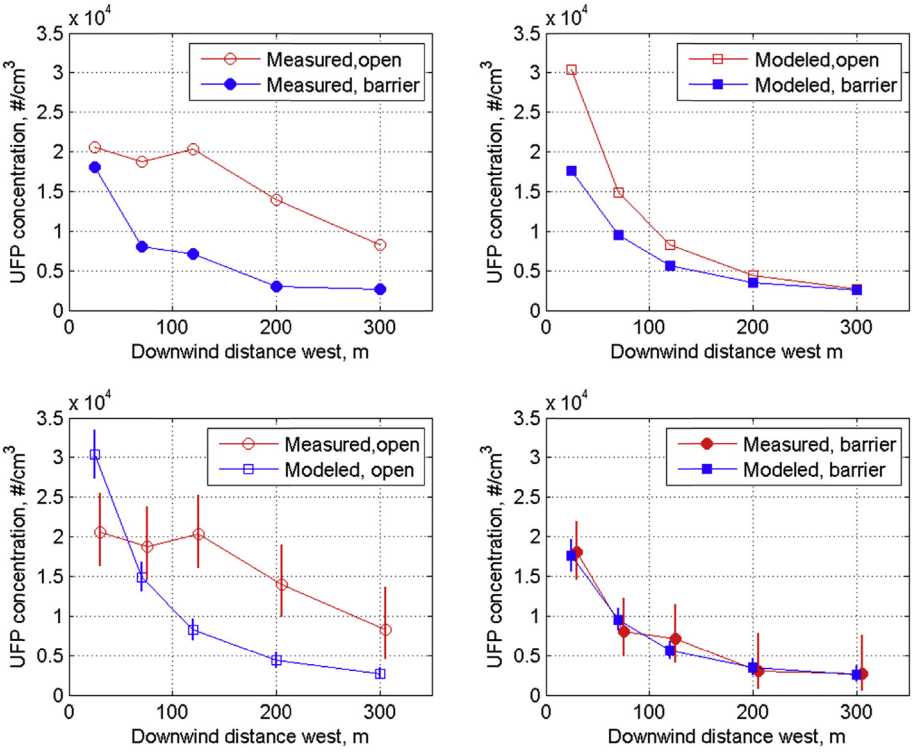

Fig. 4. Same as Fig. 3 except concentrations refer to those of ultrafine particles.

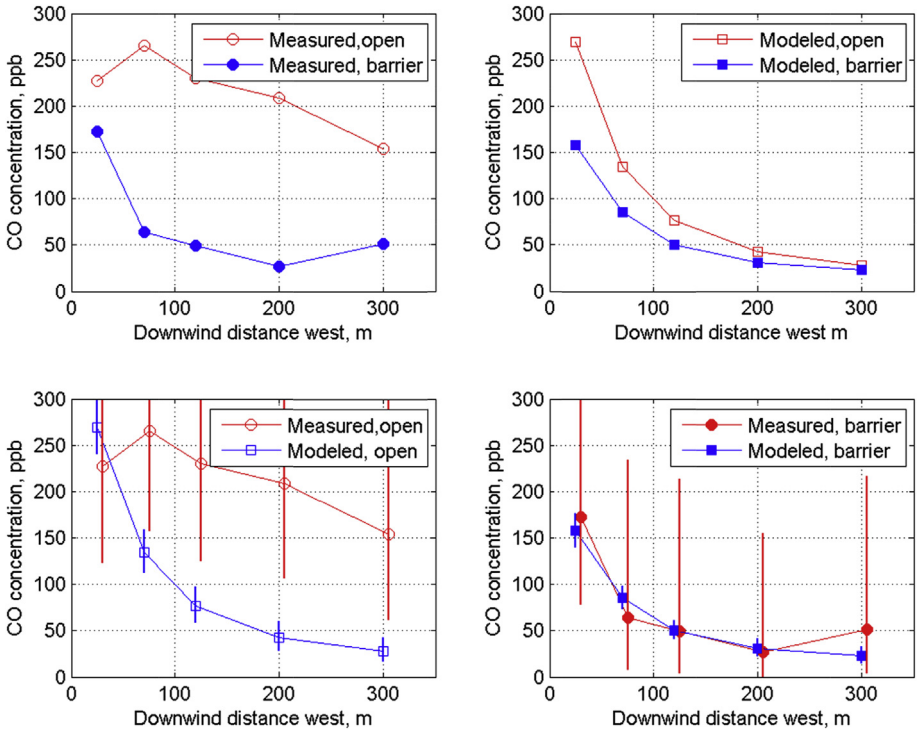

Fig. 5. Same as Fig. 3 except concentrations refer to those of CO.

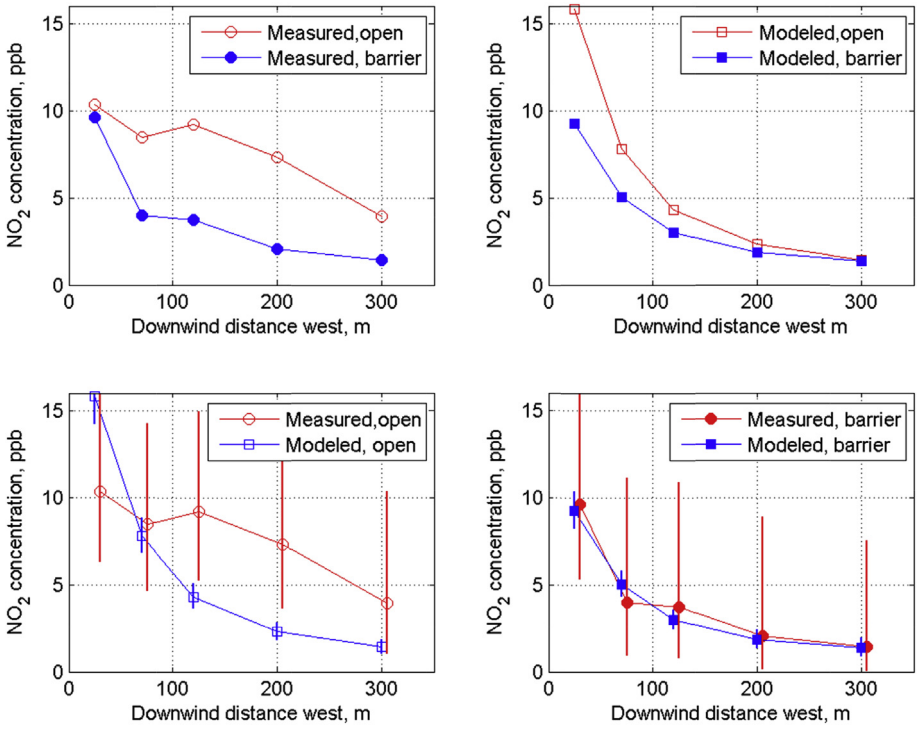

Fig. 6. Same as Fig. 3 except concentrations refer to those of NO_2.

fitting model estimates to measured concentrations, are presented in Table 1. The confidence intervals were estimated through a procedure in which 1) 1000 samples of measured and estimated means in each bin were simulated by assuming that these means are log-normally distributed about their overall means, and 2) the samples were used to generate distributions of 1000 regression coefficients, corresponding to the emission factors and background concentrations.

The emission factors for the different species are consistent with those cited in the literature (Westerdahl et al., 2012; Corsmeier

Table 1
Estimates of background concentrations and emission factors. The top number is the mean value and the bottom numbers correspond to the 95% confidence interval.

Species	Background	Emission factor
Black Carbon	0.62 $\mu g/m^3$	0.03 g/km/veh
	0.44–0.78 $\mu g/m^3$	0.02–0.04 g/km/veh
UFP	9.8×10^3 #/cm^3	3.3×10^{14} #/km/veh
	$0.84–1.11 \times 10^4$ #/cm^3	$2.6–4.0 \times 10^{14}$ #/km/veh
CO	380 ppb	3.3 g/km/veh
	345-414 ppb	1.8–5.0 g/km/veh
NO_2	15 ppb	0.32 g/km/veh
	13-16 ppb	0.2–0.45 g/km/veh

(Finn et al., 2010) during unstable conditions.

The model describes the magnitude and spatial trend of the concentrations measured downwind of the barrier; however, the model underestimates the concentrations downwind of the open section of the highway. The evidence indicates that this discrepancy is related to traffic emissions from vehicles on the arterial road to the south of the no-barrier section; there was much less traffic in the residential area downwind of the barrier section of the study area. In addition, the access road for a portion of the open section was further from the highway and elevated from the highway road surface level.

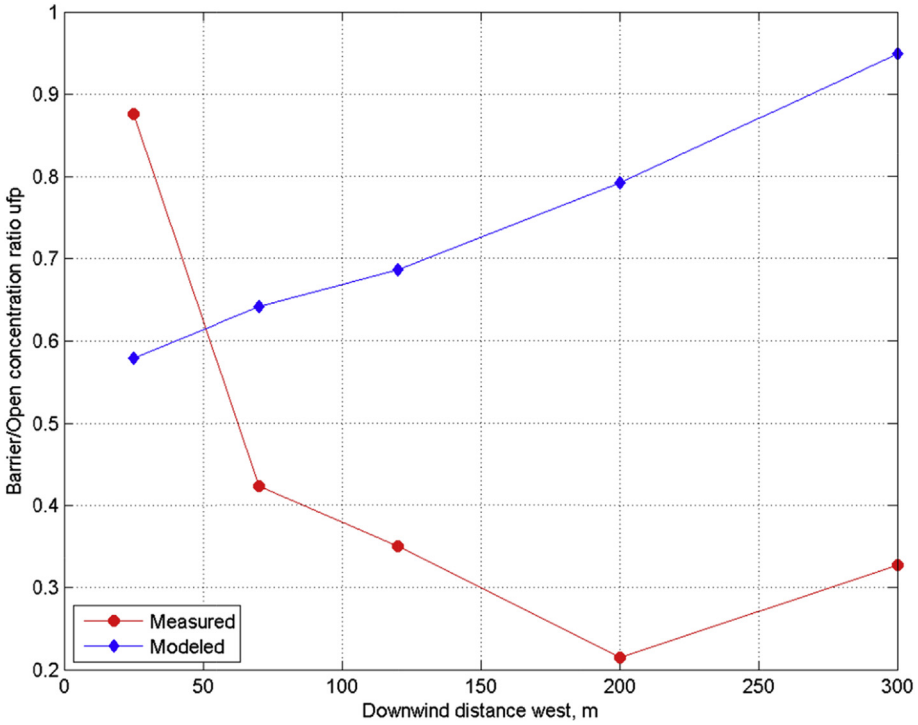

Fig. 7. Comparison of measured to modeled reductions in ultrafine particle concentrations caused by barrier.

et al., 2005). The relatively large variation in the measured concentrations of CO and NO_2 is reflected in the 95% confidence intervals of their emission factors. The emission factor for NO_2 is affected by the chemistry of NO to NO_2 conversion and thus represents an effective value.

Fig. 7 shows the ratios of concentrations measured downwind of the barrier section to those of the open section for ultrafine particle number concentrations. The modeled ratio ranges from 0.6 next to the barrier to close to unity at 300 m. The measured ratios are not representative of actual reductions because of the confounding effects of emissions and changes in terrain along the sampling path.

6. Summary and conclusions

We used a dispersion model to interpret field measurements designed to estimate the impact of noise barriers on near-road air quality in the vicinity of a major urban highway in Phoenix, Arizona, USA. The dispersion model is based on earlier work by Schulte et al. (2014) who formulated the model using data from tracer and wind tunnel studies. We modified the model to incorporate features observed in the wind tunnel and to bring the model estimates more in agreement with concentrations measured in a tracer study

We can draw three conclusions from this study: 1) We need a dispersion model, based on data from carefully controlled tracer and wind tunnel studies, to interpret real-world data, which are inevitably affected by confounding factors, 2) the presence of a solid noise barrier can reduce downwind pollutant concentrations from traffic emissions, and 3) the analysis with the model can yield useful estimates of on-road emission factors.

7. Disclaimer

This document has been reviewed in accordance with the U.S. Environmental Protection Agency policy and approved for publication. Mention of trade names or commercial products does not constitute endorsement or recommendation for use. The views expressed in this journal article are those of the authors and do not necessarily reflect the views or policies or the U.S. Environmental Protection Agency.

Acknowledgements

This study was fully funded by the U.S. Environmental Protection Agency. We thank Ben Davis and the Maricopa County Air

Quality Department for graciously providing storage and maintenance facilities for the air quality monitoring equipment. We also thank Wang Zhang and Vladimir Livshits of the Maricopa Association of Governments for traffic data on I-17 during the sampling period, and historical data on fleet mix characteristics for these sections of I-17 in Phoenix. In addition, we thank Darcy Anderson and Beverly Chenausky of the Arizona Department of Transportation for providing insights on sampling locations and assistance with permitting for access to the sampling locations. We finally want to thank Halley Brantley and Gayle Hagler for their assistance in data processing and quality assurance analyses.

References

Baldauf, R., Thoma, E., Khlystov, A., Isakov, V., Bowker, G., Long, T., Snow, R., 2008. Impacts of noise barriers on near-road air quality. Atmos. Environ. 42, 7502–7507.

Baldauf, R.W., Cahill, T.A., Bailey, C.R., Khlystov, A., Zhang, K.M., Cook, J.R., Cowherd, C., Bowker, G., 2009. Can roadway design be used to mitigate air quality impacts from traffic?. In: Air & Waste Manage Assoc. Environ. Manag. (EM), (August edition), p. 6.

Baldauf, R.W., Heist, D., Perry, S., Isakov, V., Hagler, G.S.W., Kimbrough, S., Shores, R., Black, K.N., Brixey, L., 2013. Air quality variability near a highway in a complex urban environment. Atmos. Environ. 64, 169–178.

Baldauf, R.W., Isakov, V., Deshmukh, P., Venkatram, A., 2016. Influence of solid noise barriers on near-road and on-road air quality. Atmos. Environ. 129, 265–276.

Corsmeier, U., Imhof, D., Kohler, M., Kuhlwein, J., Kurtenbach, R., Petrea, M., Rosenbohm, E., Vogel, B., Vogt, U., 2005. Comparison of measured and model-calculated real-world traffic emissions. Atmos. Environ. 39, 5760–5775.

Finn, D., Clawson, K.L., Carter, R.C., Rich, J.D., Eckman, R.M., Perry, S.G., Isakov, V., Heist, D.K., 2010. Tracer studies to characterize the effects of roadside noise barriers on near-road pollutant dispersion under varying atmospheric stability conditions. Atmos. Environ. 44, 204–214.

Hagler, G.S.W., Tang, W., Freeman, M.J., Heist, D.K., Perry, S.G., Vette, A.F., 2011. Model evaluation of roadside barrier impact on near-road air pollution. Atmos. Environ. 45, 2522–2530.

Hagler, G.S.W., Lin, M.-Y., Khlystov, A., Baldauf, R.W., Isakov, V., Faircloth, J., Jackson, L., 2012. Roadside vegetative and structural barrier impact on near-road ultrafine particle concentrations under a variety of meteorological conditions. Sci. Total Environ. 419, 7–15.

Health Effects Institute, 2010. Traffic-related Air Pollution: a Critical Review of the Literature on Emissions, Exposure, and Health Effects (Boston, MA).

Heist, D.K., Perry, S.G., Brixey, L.A., 2009. A wind tunnel study of the effect of roadway configurations on the dispersion of traffic-related pollution. Atmos. Environ. 43, 5101–5111.

Ning, Z., Hudda, N., Daher, N., Kam, W., Herner, J., Kozawa, K., Mara, S., Sioutas, C., 2010. Impact of roadside noise barriers on particle size distributions and pollutants concentrations near freeways. Atmos. Environ. 44, 3118–3127.

Schulte, N., Snyder, M., Heist, D., Venkatram, A., 2014. Effects of solid barriers on dispersion of roadway emissions. Atmos. Environ. 97, 286–295.

Venkatram, A., Horst, T., 2006. Approximating dispersion from a finite line source. Atmos. Environ. 40, 2401–2408.

Westerdahl, D., Wang, X., Pan, X., Zhang, K.M., 2012. Characterization of on-road vehicle emission factors and micro-environmental air quality in Beijing, China. Atmos. Environ. 46, 45–55.